

S²DiT: Sandwich Diffusion Transformer for Mobile Streaming Video Generation

Lin Zhao^{1,2,*} Yushu Wu^{1,2,*} Aleksei Lebedev¹ Dishani Lahiri¹ Meng Dong¹

Arpit Sahni¹ Michael Vasilkovsky¹ Hao Chen¹ Ju Hu¹ Aliaksandr Siarohin¹

Sergey Tulyakov¹ Yanzhi Wang² Anil Kag¹ Yanyu Li^{1,†}

¹Snap Inc. ²Northeastern University

* Equal contribution † Corresponding author

[Project Page](#)



Figure 1. Example results generated by our S²DiT. Our on-device model can support efficient streaming video generation.

Abstract

Diffusion Transformers (DiTs) have recently improved video generation quality. However, their heavy computational cost makes real-time or on-device generation infeasible. In this work, we introduce S²DiT—a Streaming Sandwich Diffusion Transformer designed for efficient, high-fidelity, and streaming video generation on mobile hardware. S²DiT generates more tokens but maintains efficiency with novel efficient attentions: a mixture of LinConv Hybrid Attention (LCHA) and Stride Self-Attention (SSA). Based on this, we uncover the sandwich design via a budget-aware dynamic programming search, achieving superior quality and efficiency. We further propose a 2-in-1 distillation framework that transfers the capacity of large teacher models (e.g., Wan 2.2-14B) to the compact few-step sandwich model. Together, S²DiT achieves quality on par with state-of-the-art server video models, while streaming at over 10 FPS on an iPhone.

1. Introduction

Diffusion Transformers (DiTs) [15, 36, 40, 56] have rapidly advanced the frontier of video generation, achieving state-of-the-art quality in both foundational text/image to video generation and downstream tasks such as video editing, up-sampling and frame interpolation [8, 41, 44, 57].

Despite the rapid progress, several major bottlenecks still remain, particularly in inference speed and resource efficiency. A key source of the limitations lies in the quadratic computational complexity and memory footprint of the attention mechanism over a large number of tokens, which fundamentally hinder real-time and on-device generation. Recent works have explored the efficiency of video DiT, e.g., LTX [11], SnapGenV [46], SnapGenV-DiT [45], SANA Video [3]. They mostly rely on high-compression video VAEs to obtain a compact latent space [10, 45], but struggle to match the visual fidelity and temporal coherence of top-tier large-scale models due to the significantly reduced token count. Meanwhile, streaming video genera-

tion models [16, 25, 53] have drawn increasing attention because of their on-the-fly and interactive generation capabilities. Such models impose higher demands on real-time, on-device generation compared to the base bidirectional models [19, 45, 46], yet mobile deployment remains largely underexplored. The open problem is that: *How to achieve high fidelity, mobile-efficient, and streaming-capable video generation simultaneously?*

In this work, we propose S²DiT, a Sandwich diffusion transformer for mobile Streaming video generation as presented in Fig. 1. We address the challenge from two aspects.

An Efficient Sandwich Diffusion Transformer. To overcome the quadratic cost of conventional self-attention in DiTs, we design a multi-stage “sandwich” DiT architecture that interleaves two efficient attention modules. The LinConv Hybrid Attention (LCHA) combines a learnable positive-kernel linear path with a depthwise 3D convolution path, achieving linear complexity while preserving spatiotemporal fidelity. The Stride Self-Attention (SSA) compresses intermediate feature maps to improve throughput. Based on this, we propose a dynamic programming-based search algorithm that determines the placement of LCHA and SSA modules by optimizing their allocation under latency and memory constraints. The resulting Sandwich DiT achieves superior quality and speed compared to multiple ablated alternatives, offering a strong backbone for mobile video generation.

2-in-1 Distillation Pipeline. Building upon the architecture, we introduce a 2-stage distillation pipeline guided by 1 single teacher model, enabling high-fidelity generation with limited computational budgets. After achieving training convergence, we first perform cached offline knowledge distillation from a large-scale teacher model (i.e., Wan 2.2-14B). Instead of relying on expensive on-the-fly teacher inference, we precompute and cache diffusion tuples and text embeddings from the teacher models, enabling cost-efficient supervision of the student model. This protocol preserves semantic consistency while substantially reducing training FLOPs and peak memory, effectively transferring the visual quality of billion-scale models to a compact mobile backbone.

For the second stage, we extend our framework to streaming video generation through the self-forcing strategy [16]. We employ step distillation to shorten the denoising trajectory, leveraging distribution matching distillation with the same large-scale teacher model used in the first stage. In addition, we explore adversarial fine-tuning to enforce temporal coherence across streaming segments under a few sampling steps. The resulting model can synthesize videos in an online, causal manner, maintaining frame-to-frame consistency while achieving high-speed generation on mobile devices. To our knowledge, this is the first diffusion transformer enabling on-device streaming video generation

Model	VBench	Mobile	Mobile Streaming
Wan2.1-1.3B [40]	83.31	✗	✗
LTX-2B [10]	80.00	✗	✗
SnapGenV [46]	81.14	5s / 4s	✗
Mobile-DiT [45]	81.45	5s / 4s	✗
NeoDragon [19]	81.61	2s / 6.7s	✗
S ² DiT-AR	83.26	✓	~ 11 FPS

Table 1. We present S²DiT, the first-ever mobile streaming video generation model with comparable quality to best server ones. For methods that support mobile deployment, we report video length / latency.

with both high fidelity and low latency as shown in Tab. 1. Our contributions can be summarized as follows:

- We propose S²DiT, a streaming sandwich-like diffusion transformer that interleaves two efficient attention modules—hybrid linear-local attention (LCHA) and Stride Self-Attention (SSA), to balance global and local modeling under mobile constraints. In addition, we propose a dynamic programming-based search algorithm that automatically allocates LCHA and SSA to optimize the latency-fidelity trade-off.
- We introduce a 2-in-1 distillation framework for S²DiT that transfers the high-fidelity generation capability of large-scale teacher models (e.g., Wan 2.2-14B) to the compact, few-step sandwich transformer, yielding an efficient auto-regressive video diffusion model.
- We are the first to demonstrate high-fidelity, high-dynamic, and high-speed streaming video generation on a mobile device.

2. Related Works

Video Diffusion Models. In recent years, video generation models have advanced rapidly [22–24, 27, 30, 37, 39, 51]. Most progress has centered on large diffusion models that iteratively denoise Gaussian noise into real videos conditioned on text or image inputs. These methods encompass both pixel-space approaches [14, 28] and latent-space variants [39, 51]. Although systems such as [10, 28, 30, 31, 51, 56] can produce highly realistic videos, their substantial compute and memory footprint limits their practicality for on-device deployment.

Mobile Deployment. Relatively few works have explored on-device video generation [21, 46]. Although Wan2.1 [39] offers 1.3B T2V model, it has a high number of tokens for on-device inference due to low VAE compression. LTX-Video [9] employs a highly compressed VAE with a 1.9B DiT, although runs in real-time on GPUs, it remains impractical for mobile devices. Mobile Video Diffusion [50] simplifies Stable Video Diffusion [2] by pruning channels and blocks. SnapGen-V [46] compromises visual quality due to a low-capacity lightweight UNet architecture. On-device Sora [21] enables low-resolution video generation on iPhones by merging temporal tokens and dynamically loading blocks to alleviate memory constraints.

Streaming Video Generation Several recent works have specifically tackled the challenge of streaming or causal video generation rather than the conventional full-sequence (bidirectional) diffusion approach. For example, CausVid [53] introduces an auto-regressive diffusion transformer by converting a pretrained bidirectional backbone into one that generates frames on the fly, achieving real-time streaming (9.4 FPS) through key-value caching and a distribution-matching distillation from 50 steps to 4 steps. Self-forcing [16] mitigates exposure bias in auto-regressive video diffusion by simulating inference at training time—performing self-rollouts, conditioning on model-generated context, and applying a holistic video-level loss—thus enabling sub-second latency streaming on a single GPU. AAPT [25] proposes an adversarial post-training method that transforms a pretrained latent video diffusion model into a real-time interactive streamer, enabling one latent frame per network forward evaluation and supporting long-duration (*e.g.*, 1 minute+) streaming at 24 fps with low latency.

3. Method

3.1. Design Overview

Unlike prior mobile video diffusion systems that rely on extremely compressed latent spaces, S²DiT operates in a moderately compressed latent representation that preserves more spatial and temporal detail. This choice improves fidelity but significantly increases the number of latent tokens, making conventional DiT architectures too slow for mobile deployment.

Our approach addresses this challenge through a structured architectural pattern that alternates high-resolution and low-resolution processing stages. At a high level, Sandwich DiT interleaves two complementary attention modules: LinConv Hybrid Attention (LCHA) for high-resolution modeling that preserves detail at linear cost, and Stride Self-Attention (SSA) for low-resolution modeling that aggregates global context at reduced token count. The architectural layout and the precise allocation of these modules are determined through a budget-aware search.

In addition, distillation from a powerful teacher model plays a central role, supplying rich semantic and structural guidance that leads to better visual quality and motion consistency. On top of Sandwich DiT, we introduce a two-in-one distillation pipeline that (i) aligns the student with a strong teacher model (Wan2.2) through offline cached distillation, and (ii) incorporates Distribution-Matching Distillation (DMD) and self-forcing to support few-step auto-regressive generation.

3.2. Efficient Attention

To address the computation burden from the large latent space, we perform a systematic investigation on mobile-

friendly efficient attention mechanisms. There are two major directions to reduce attention complexity, (i) reduce the quadratic complexity of self-attention by swapping to linear attention, and (ii) introduce token sparsity.

3.2.1. LinConv Hybrid Attention (LCHA)

Unlike conventional Softmax attention, Linear attention [20] approximates the similarity function with a non-negative kernel which applies to queries and keys separately, which can be expressed as:

$$y_i = \frac{\sum_{j=1}^L \phi(q_i)^\top \phi(k_j) v_j}{\sum_{j=1}^L \phi(q_i)^\top \phi(k_j)} \quad \text{with } \phi(\cdot) \geq 0,$$

where L is the sequence length, q_i, k_j are the query and key vectors at positions i and j , and v_j is the corresponding value. According to associativity, we can then compute $\sum_{j=1}^L \phi(k_j) \cdot v_j^\top$ first, such that computation is linear to the number of tokens. But as discussed in [12, 33], linear attention shows inferior modeling capability compared to full attention, and is more global but coarse in local information modeling. To address this, we propose a hybrid attention module that achieves linear computational complexity but captures both global and local dependency well. As in Fig. 2, the module consists of two branches:

Linear Attention Path. We introduce an optimized linear attention module. Specifically, instead of using ReLU as the similarity kernel [4, 49], we use a learnable positive kernel:

$$\begin{aligned} K(q, k) &= \phi(q)^\top \phi(k), \\ \phi(x) &= \text{softplus}(Wx + b). \end{aligned} \quad (1)$$

This choice guarantees $\phi(x) > 0$, and the softplus preserves information for negative inputs and maintains non-vanishing gradients. We learn affine parameters (W, b) end-to-end, allowing the feature map to adapt dynamically to distributional variation to improve the quality. Different from [48], we apply QK normalization [13] and 3D RoPE embedding [35], which were not used in their design.

Local Conv Path. We augment the linear attention building block with a convolution path to enrich local detail modeling. Specifically, we employ a depth-wise 3D convolution followed by a linear channel mixing layer as a parallel branch. To support streaming generation, we apply temporal causal padding to the depth-wise 3D convolution. According to our benchmark, dense 3D convolution will lead to OOM for mobile deployment.

We use a learnable gate α (denoted as FusionGate) to mix the output of the two branches. We include extensive ablation experiments in Sec. 4.4.1 to validate the effectiveness of the proposed LinConv Hybrid Attention (LCHA).

3.2.2. Stride Self-Attention (SSA)

Another route to efficient attention is token sparsity. From the scope of mobile support, only structured sparsity is

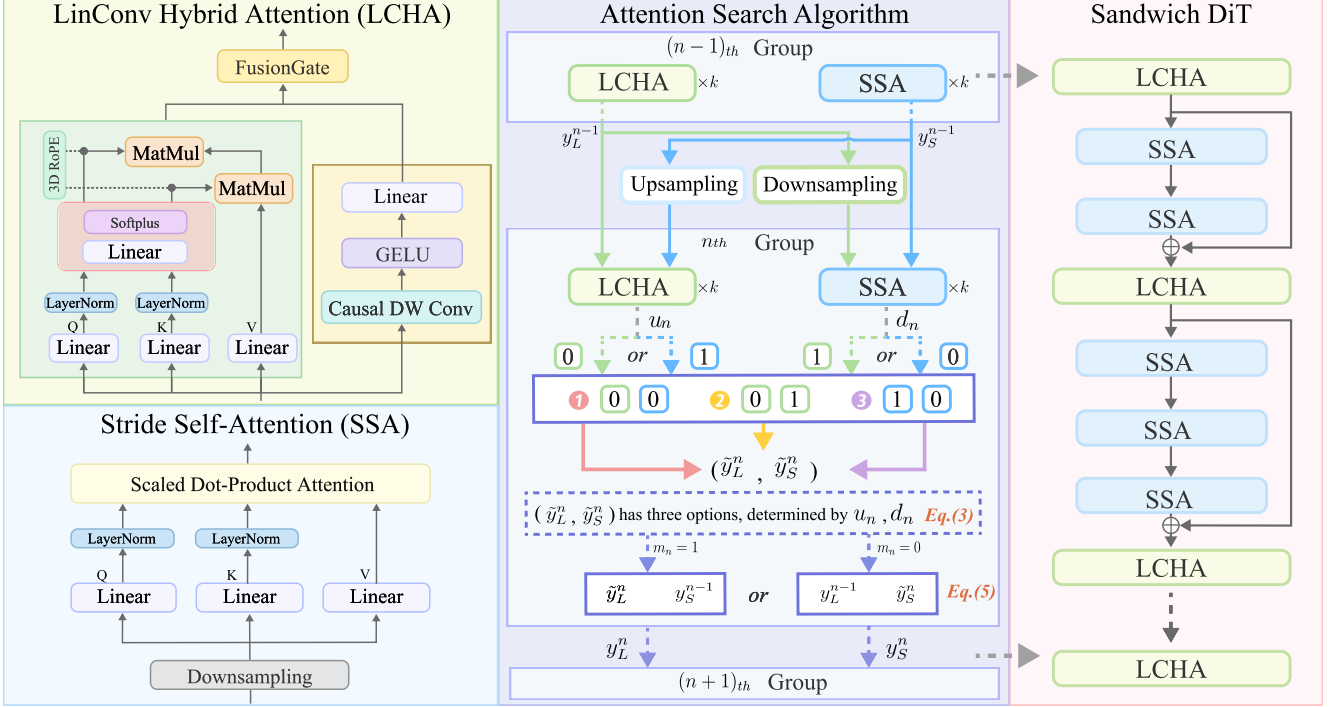


Figure 2. **Illustration of the framework for obtaining S^2 DiT.** LCHA integrates a linear attention path with a local convolution path at high resolution, while SSA compresses the spatial representation for efficient global context modeling. The final S^2 DiT is derived by combining these two efficient attention designs with the attention search algorithm.

of-interest in our case, while random or dynamic sparsity (sliding window) requires dedicated compilation, which is not yet supported. In this work, we investigate uniform KV sparsity (KV compression) and uniform QKV sparsity (stride self-attention). Among them, KV compression is a widely adopted strategy to reduce the cost of attention matrix multiplication while keeping the same output tokens [26, 43]. On the other hand, we can uniformly downsample QKV with certain strides, which requires an upsampling to restore the feature resolution. Note that empirically, using strided attention for all DiT blocks is equivalent to a low-resolution DiT, *i.e.*, DiT on a higher compression latent space [10, 45].

In our ablation study at Sec. 4.4.1, we show that KV compression is inefficient, while relying solely on low-resolution SSA significantly degrades generation quality. Therefore, we employ the hybrid design that combines SSA with LCHA. The two types of attention modules feature an elegant speed/quality trade-off, and provide a complementary design space that enables effective architecture search under mobile compute budgets.

3.3. Sandwich Diffusion Transformer

With the LCHA and SSA building blocks, we propose an automatic distribution search algorithm to form the final architecture. Compared to simple heuristics such as HDiT [6],

which places low-resolution blocks in the middle to form a U-connected architecture, our automatically searched architecture distributes LCHA and SSA in an interleaved manner, as in Fig. 2. Our final model, Sandwich DiT, achieves higher performance compared to the HDiT architecture, which can be seen in Sec. 4.4.2.

3.3.1. Budget-aware Block Allocation.

We first determine the counts of LCHA and SSA blocks via a budget-aware dynamic programming that satisfies the target latency and memory constraints. Let $t \in \{\text{LCHA}, \text{SSA}\}$ denote the block type, where each transformer block employs the corresponding proposed attention. Each type of block is associated with a latency ℓ_t and memory consumption m_t . We choose non-negative integers N_t such that satisfies with capacity $N_{\text{LCHA}} + N_{\text{SSA}} = K$, where K is the total number of blocks, subject to a $\sum_t \ell_t N_t \leq L_{\max}$, and a peak-memory budget $\sum_t m_t N_t \leq M_{\max}$.

To fully utilize the compute budget of the target device, we select the $(N_{\text{LCHA}}, N_{\text{SSA}})$ pair whose resulting (L, M) is closest to (L_{\max}, M_{\max}) .

3.3.2. Attention Search Algorithm.

Once the block counts of each type are fixed, we search for the optimal distribution of LCHA and SSA blocks to construct the final architecture.

Problem Formulation. We partition the search space \mathcal{G} into M groups $\{\mathcal{G}_n\}_{n=1}^M$, each contains k blocks with LCHA or SSA. At group n , a binary mask $m_n \in \{0, 1\}$ routes computation to the LCHA ($m_n=1$) or SSA ($m_n=0$). We maintain two feature streams, y_L^n and y_S^n , and a buffer S^n that caches the residual feature for long-skip connection. Let $f_L^n(\cdot)$ and $f_S^n(\cdot)$ denote the n -th group of modules for the two branches, respectively. Our goal is to learn m_n that decides between $f_L^n(\cdot)$ or $f_S^n(\cdot)$ for each $n \in \{1, \dots, M\}$, yielding the optimal composition across groups.

Branch-Switch Triggers. Since the two attention branches operate at different spatial resolutions, cross-branch routing at stage n applies upsampling $up_n(\cdot)$ and downsampling $down_n(\cdot)$ as needed. We gate this choice with binary triggers u_n and d_n like following:

$$\begin{aligned} u_n &= \max\{m_n - m_{n-1}, 0\}, \\ d_n &= \max\{m_{n-1} - m_n, 0\}. \end{aligned} \quad (2)$$

Thus, $u_n = 1$ if routing switches from y_S^{n-1} to y_L^n , and $d_n = 1$ if it switches from y_L^{n-1} to y_S^n , otherwise $u_n = d_n = 0$.

Per-group Differentiable Updating. As shown in Fig. 2, we first compute the switching results of both branches based on our definition:

$$\begin{aligned} \tilde{y}_L^n &= f_L^n\left((1 - u_n) y_L^{n-1} + u_n (up(y_S^{n-1}) + S^{n-1})\right), \\ \tilde{y}_S^n &= f_S^n\left((1 - d_n) y_S^{n-1} + d_n down(y_L^{n-1})\right) \end{aligned} \quad (3)$$

where \tilde{y}_L^n and \tilde{y}_S^n are the switching results. Besides, we update S^n only at LCHA \rightarrow SSA, which can be formulated as following:

$$S^n = d_n y_L^{n-1} + (1 - d_n) S^{n-1}. \quad (4)$$

Finally, m_n determines whether each stream is updated. we apply the Gumbel-Softmax function [18] combined with the Straight-Through Estimator for the m_n updating:

$$\begin{aligned} y_L^n &= m_n \tilde{y}_L^n + (1 - m_n) y_L^{n-1}, \\ y_S^n &= (1 - m_n) \tilde{y}_S^n + m_n y_S^{n-1}. \end{aligned} \quad (5)$$

After the last group M , the output feature \hat{y} is:

$$\hat{y} = m_M \cdot y_L^{(M)} + (1 - m_M) \cdot up(y_S^{(M)}). \quad (6)$$

The details of our efficient search space and training design are in the *supplementary materials*.

3.4. 2-in-1 Distillation

Preliminaries. Our base model training follows the Rectified Flow [42] objective. The forward path is a straight line from the data distribution x_0 to standard Gaussian noise

$\epsilon \sim \mathcal{N}(0, I)$, the noisy sample x_t at timestep $t \in [0, 1]$ can be expressed as:

$$x_t = (1 - t) x_0 + t \epsilon \quad (7)$$

Along this path, the target velocity is $\epsilon - x_0$. We train our model v_θ to predict this velocity from (x_t, t) via:

$$\mathcal{L}_{\text{fm}} = \mathbb{E}_{\epsilon \sim \mathcal{N}(0, I), t} \left[\|(\epsilon - x_0) - v_\theta(x_t, t)\|_2^2 \right]. \quad (8)$$

Offline Cached Knowledge Distillation. Inspired by [7, 45], we employ knowledge distillation as a final refinement stage to further improve S²DiT after the architecture search and pretraining. To enable effective knowledge transfer, we align the student and the teacher model by training both within an identical VAE latent space, and optimize the student to match the teacher’s outputs under identical conditioning and noise levels. Given that high quality video diffusion models like Huanyuan Video [22] (13B parameters) are impractically large and slow, requiring dozens of seconds for a single forward pass, an on-the-fly distillation approach is infeasible.

To address this issue, we introduce *Offline Cached Knowledge Distillation*, a protocol that decouples teacher inference from student training by using precomputed, cached teacher outputs. The cached data significantly improves training throughput and allows for larger batch sizes, which benefit convergence of the student model. The proposed distillation pipeline consists of two stages: (i) Precompute and cache the noisy latents of real data, text embeddings, timestep and teacher model’s output predictions. (ii) Perform distillation solely using the cached data, eliminating the need of real data, the text encoder, or teacher model during this stage. The distillation loss can be formulated as:

$$\mathcal{L}_{\text{KD}} = \mathbb{E} \left[\|u_{\theta_s}(x_t, t, c_{\text{text}}) - u_{\theta_t}(x_t, t, c_{\text{text}})\|_2^2 \right], \quad (9)$$

where u_{θ_s} is the student model, x_t is noisy latent of timestep t , c_{text} is corresponding text embeddings, and $u_{\theta_t}(x_t, t, c_{\text{text}})$ is cached teacher output under the identical input. Specifically, we adopt Wan2.2-14B [40] as the teacher model due to its superior visual fidelity.

Distillation for Streaming. Prior works such as APT2 [25] and Self-Forcing [16], address the training inference mismatch caused by teacher-forcing when generating video auto-regressively. Following these approaches, we adopt distribution matching distillation (DMD) to adapt the knowledge-distilled S²DiT for auto-regressive (chunk-level) video generation. Before self-forcing, we collect the ODE trajectory of S²DiT and perform teacher-forcing fine-tuning on bidirectional S²DiT to obtain well-initialized generator weights. During self-forcing DMD training, the real-score model is initialized from the same teacher as knowledge distillation (*i.e.* Wan2.2-14B), while the fake-score model is initialized from the knowledge-distilled S²DiT.

We also explore adversarial fine-tuning on top of the self-

forcing DMD training. Details are discussed in the *supplementary materials*.

Streaming Inference on Mobile. Thanks to the state inheritance, the causal inference in the Linear Attention and Causal Conv3D layers of the LCHA block requires only a fixed-size cache. In contrast, although the SSA block reduces the sequence length via a downsampling layer, its KV-cache still grows with the number of generated frames, leading to substantial memory overhead during mobile deployment. To alleviate this issue, we apply window attention to the KV-cache, which both accelerates the inference speed and mitigates memory accumulation.

With DMD-based self-forcing fine-tuning, our model achieves efficient auto-regressive inference with fewer than 4-step per frame-chunk, enabling on-device, streaming video generation. Additional implementation and analysis details are available in the *supplementary materials*.

4. Experiments

4.1. Setup

Data. Following [5, 40, 58], we collect image and video data from both public and internal sources. After applying safety filters and quality filters (*e.g.*, aesthetics, motion score), we arrive at a total of 300M images and 50M videos.

Model Pipeline. To achieve best generation quality, we employ the SOTA Wan Autoencoder with $4 \times 8 \times 8$ compression ratio. We further create an efficient decoder for mobile deployment, as detailed in *supplementary material*. Similar to previous work [48], we employ CLIP-ViT-L [34] and Gemma3-4B-it [38] as the text encoder. CLIP serves as the efficient mobile model, while Gemma3 provides strong contextual information with prompt augmentation on-the-fly. We adopt the UniPC sampler [55] following Wan2.1 [40].

Training Details. Following progressive training [40], our model is first pretrained on low resolution data for faster convergence, then scaled up to high resolution pretraining and knowledge distillation. We train 250K iterations at 256×144 stage, and 50K iterations at 512×288 stage. Training is conducted on 256 NVIDIA A100 (80GB) GPUs using the AdamW optimizer with a learning rate of 1×10^{-4} and $\beta = [0.9, 0.999]$.

Evaluation. We compare Vbench score with popular video diffusion models. For ablation studies, we report the evaluation loss with 50 sampling steps, CLIP score, FID, FVD. We also include a user study in the *supplementary material*.

Deployment. We use CoreMLTools [1] to deploy the model to iPhone 16 Pro Max for speed benchmark and demonstration. We provide details in *supplementary material*.

4.2. Qualitative Results

We conduct a visual comparison of video samples generated by LTX-Video, Wan2.1-1.3B, S²DiT (Pre-trained), S²DiT (Knowledge-Distilled), and S²DiT (Auto-Regressive) in Fig. 3. As illustrated, S²DiT variants deliver superior video quality in terms of text-video alignment, photorealistic rendering, and smooth object motions compared to LTX-Video with heavily compressed latent space, while being comparable to Wan2.1-1.3B. With knowledge distillation, S²DiT-(KD) produces vivid videos that surpass the quality of Wan2.1-1.3B. The auto-regressive (AR) variant achieves comparable visual fidelity to S²DiT-(KD), while requiring fewer sample steps and supporting efficient on-device streaming generation. More visualizations are included in the *supplementary material*.

4.3. Quantitative Results

We compare against recent open-source SOTA models, including LTX-Video, CogVideoX, Open-Sora, Wan2.1, and Hunyuan. Despite using only 1.8B parameters, S²DiT-(KD) attains a total Vbench of 83.62, on par with Hunyuan-13B and Open-Sora-2.0, and close to Wan2.1-14B. Our models also achieve strong Quality scores. For fast inference, the S²DiT-(AR) reaches 83.26 while maintaining competitive fidelity, making it suitable for mobile deployment. Besides, by comparing the three versions, S²DiT-(KD) and S²DiT-(AR) get better results than S²DiT-(Pretrained), which verifies the benefits of our proposed 2-in-1 Distillation in Sec. 3.4.

4.4. Ablation Study

4.4.1. Impact of Efficient Attention Design.

We present an extensive ablation study that validates our efficient-attention design in Tab. 3. For this purpose, we randomly select 2,000 videos from the OpenVid dataset [29] that are disjoint from our training data. The subset is utilized for the below ablations. All variants are pre-trained under a matched compute budget and training schedule to ensure a fair comparison.

Flat-attention variants. We begin by assessing the variants in a single-stage setting as shown in the *top block* of Tab. 3: (i) Full Attention: We set all blocks to standard self-attention. As shown in Tab. 3, this variant obtains the highest quality but is the most computationally expensive, owing to its quadratic complexity and full token budget. It can be seen as the upper-bound of our design, since our method serves as an efficient approximation. (ii) LCHA-only: to assess the effect of the multi-stage design with mixing LCHA and SSA, we fix the attention to LCHA in all blocks. (iii) SSA-only: similarly, we set all blocks to SSA for comparison, which reduces the token count by 4 \times and thus sacrifices the model capacity. As expected, this configuration



Figure 3. **Visual comparisons.** For Wan-1.3B [40] and LTX-2B [10], videos are generated using their official default inference resolutions with the same prompts.

yields the weakest quality and serves as the lower-bound for our model.

It shows that our result lies substantially closer to the upper-bound than the lower-bound across all metrics. LCHA-only outperforms SSA-only across all metrics, indicating the importance of a high-resolution stage for generation. Besides, our two-stage model further surpasses LCHA-only on Eval loss, FID, and FVD, indicating that combining high-resolution modeling (LCHA) with low-resolution global context (SSA) yields the best results.

Our Linear Attention vs. KV Compression. Beyond linear attention, key-value (KV) compression is also effective on mobile, as discussed in Sec. 3.2.2. Accordingly, we convert the linear attention path in LCHA with a KV compression variant, enabling a direct comparison to our proposed linear attention. We evaluate both a one-stage model using KV compressed LCHA and a two-stage hourglass model combining KV compressed LCHA with SSA similar to our setting. As shown in the *middle block* of Tab. 3, the one-stage KV-Compression version is slightly better than

Model	Params (B)	Total	Quality	Semantic	Flickering	Aesthetics	Imaging	Obj. Class	Scene	Consistency
Hunyuan	13	83.24	85.09	75.82	99.44	60.36	67.56	86.10	53.88	26.44
Open-Sora-2.0	11	84.34	85.40	80.12	99.40	64.39	65.66	94.50	52.71	27.50
Open-Sora-1.2	1.2	79.76	81.35	73.39	99.53	56.85	63.34	82.22	42.44	26.85
Wan2.1	14	84.70	85.64	80.95	99.53	61.53	67.28	94.24	53.67	27.44
Wan2.1	1.3	83.31	85.23	75.65	99.55	65.46	67.01	88.81	41.96	25.50
CogVideoX1.5	5	82.01	82.72	79.17	98.53	62.07	65.34	83.42	53.28	27.42
CogVideoX	5	81.91	83.05	77.33	78.97	61.88	63.33	85.07	51.96	27.65
LTX-Video	1.8	80.00	82.30	70.79	99.34	59.81	60.28	83.45	51.07	25.19
SnapGen-V-DiT	0.9	81.45	83.12	74.76	98.11	64.16	63.41	92.26	51.06	25.51
S^2 DiT-Pretrained	1.8	82.40	84.41	74.46	98.52	64.97	68.49	91.74	44.35	24.94
S^2 DiT-KD	1.8	83.62	86.13	73.58	99.56	65.26	69.05	91.76	48.37	25.35
S^2 DiT-AR†	1.8	83.26	85.63	73.79	98.20	65.64	70.57	89.49	49.19	24.75

Table 2. **VBench [17] comparisons.** Scores for open-source models are collected from the [VBench Leaderboard](#). † Tested with mobile deployment resolution (512×288), other S^2 DiT results are reported in higher resolution (480×832) to better compare with baselines.

Method	Latency↓	Eval loss↓	CLIP↑	FID↓	FVD↓
Full Attention	OOM	0.252	0.281	32.035	317.130
SSA-only	258	0.269	0.263	37.529	377.209
LCHA-only	900	0.259	0.270	33.185	339.380
KV-Comp.-only	1348	0.255	0.275	32.609	333.473
KV-Comp. + SSA	736	0.257	0.273	32.912	337.128
Local path-only	347	0.263	0.268	33.846	349.381
Linear path-only	457	0.265	0.269	36.448	357.473
PSoftplus→ReLU	499	0.258	0.270	33.373	336.984
LinAtt dim 128→256	569	0.259	0.267	34.112	352.188
w.o. FusionGate	527	0.256	0.271	32.897	332.170
Sandwich DiT	531	0.256	0.272	32.209	330.978

Table 3. **Ablation of Our Efficient Attention Design**. Latency is benchmark on iPhone 16 Pro Max. **OOM** indicates out-of-memory.

LCHA-only. However, based on the latency comparison, linear version get benefit compared to the kv-compression version. For the two-stage model, linear version get a better result.

Ablation of LCHA. Furthermore, we individually disable each proposed component to isolate its contribution in the LCHA design as demonstrated in the *bottom block* of Tab. 3. Removing either the linear path or the local path degrades quality. However, the local-only variant outperforms the linear-only variant, consistent with our hypothesis in Sec. 3.2.1 that DiT-based models rely more heavily on local information. We replace the PSoftplus mapping (linear + softplus) with a ReLU variant and observe worse FID/FVD, indicating that PSoftplus yields better perceptual quality. We vary the head dimension d_h of linear attention and observe that $d_h = 256$ performs worse than $d_h = 128$. In addition, adding FusionGate yields a small but consistent improvement. Our comprehensive experiments confirm that every component of LCHA is effective and synergistically contributes to the observed improvements.

Model	Res	$\mathcal{L}_{\text{eval}} \downarrow$	CLIP ↑	FID ↓	FVD ↓
Full Attention	288p	0.180	0.294	26.495	130.825
SSA-only	288p	0.283	0.286	36.788	221.390
Hourglass	288p	0.220	0.290	30.697	167.094
Sandwich	288p	0.209	0.291	29.565	145.297

Table 4. **Comparison of different architecture on 512×288 resolution.**

4.4.2. Impact of Sandwich Architecture.

To assess the effectiveness of the proposed attention distribution search algorithm, we compare our Sandwich DiT with the Hourglass DiT under the same setting at 512×288 resolution. The 512×288 models are obtained by fine-tuning from 256×144 models. As illustrated in Tab. 2, Sandwich DiT consistently outperforms the hourglass variant across metrics at both resolutions.

We further benchmark Full Attention (upper-bound) and SSA-only (lower-bound) at 512×288 . Both hourglass and sandwich versions are closer to the upper-bound, consistent with Sec. 4.4.1, indicating that our design performs well at both low and high resolutions.

5. Conclusion

We presented S^2 DiT, a Streaming Sandwich Diffusion Transformer that unifies architectural search, efficient training, and self-forcing inference for mobile video generation. By alternating hybrid linear-local and strided attention modules and optimizing their allocation through dynamic programming, S^2 DiT achieves an exceptional balance between quality and latency. Our offline cached knowledge distillation pipeline enables compact students to inherit the fidelity of large-scale teachers at a fraction of the cost, combined with self-forcing, we further extend the model to real-time, auto-regressive video synthesis. Together, these designs push diffusion transformers beyond the server environment, demonstrating that high-quality streaming generation is achievable on mobile.

References

[1] Apple Inc. Core ML Tools. <https://coremltools.readme.io/>, 2024. Version 8.0, accessed on September 7, 2025. 6, 2

[2] Andreas Blattmann, Tim Dockhorn, Sumith Kulal, Daniel Mendelevitch, Maciej Kilian, Dominik Lorenz, Yam Levi, Zion English, Vikram Voleti, Adam Letts, et al. Stable video diffusion: Scaling latent video diffusion models to large datasets. *arXiv preprint arXiv:2311.15127*, 2023. 2

[3] Junsong Chen, Yuyang Zhao, Jincheng Yu, Ruihang Chu, Junyu Chen, Shuai Yang, Xianbang Wang, Yicheng Pan, Daquan Zhou, Huan Ling, Haozhe Liu, Hongwei Yi, Hao Zhang, Muyang Li, Yukang Chen, Han Cai, Sanja Fidler, Ping Luo, Song Han, and Enze Xie. Sana-video: Efficient video generation with block linear diffusion transformer. 2025. 1

[4] Junsong Chen, Yuyang Zhao, Jincheng Yu, Ruihang Chu, Junyu Chen, Shuai Yang, Xianbang Wang, Yicheng Pan, Daquan Zhou, Huan Ling, et al. Sana-video: Efficient video generation with block linear diffusion transformer. *arXiv preprint arXiv:2509.24695*, 2025. 3

[5] Tsai-Shien Chen, Aliaksandr Siarohin, Willi Menapace, Ekaterina Deyneka, Hsiang-wei Chao, Byung Eun Jeon, Yuwei Fang, Hsin-Ying Lee, Jian Ren, Ming-Hsuan Yang, and Sergey Tulyakov. Panda-70m: Captioning 70m videos with multiple cross-modality teachers. In *Proceedings of the IEEE/CVF Conference on Computer Vision and Pattern Recognition*, 2024. 6

[6] Katherine Crowson, Stefan Andreas Baumann, Alex Birch, Tanishq Mathew Abraham, Daniel Z Kaplan, and Enrico Shippole. Scalable high-resolution pixel-space image synthesis with hourglass diffusion transformers. *arXiv preprint arXiv:2401.11605*, 2024. 4

[7] Gongfan Fang, Kunjun Li, Xinyin Ma, and Xinchao Wang. Tinyfusion: Diffusion transformers learned shallow. *arXiv preprint arXiv:2412.01199*, 2024. 5

[8] Yuwei Guo, Ceyuan Yang, Anyi Rao, Yaohui Wang, Yu Qiao, Dahua Lin, and Bo Dai. Animatediff: Animate your personalized text-to-image diffusion models without specific tuning. *arXiv preprint arXiv:2307.04725*, 2023. 1

[9] Yoav HaCohen, Nisan Chiprut, Benny Brazowski, Daniel Shalem, Dudu Moshe, Eitan Richardson, Eran Levin, Guy Shiran, Nir Zabari, Ori Gordon, Poriya Panet, Sapir Weissbuch, Victor Kulikov, Yaki Bitterman, Zeev Melumian, and Ofir Bibi. Ltx-video: Realtime video latent diffusion. 2024. 2

[10] Yoav HaCohen, Nisan Chiprut, Benny Brazowski, Daniel Shalem, Dudu Moshe, Eitan Richardson, Eran Levin, Guy Shiran, Nir Zabari, Ori Gordon, et al. Ltx-video: Realtime video latent diffusion. *arXiv preprint arXiv:2501.00103*, 2024. 1, 2, 4, 7, 3

[11] Yoav HaCohen, Nisan Chiprut, Benny Brazowski, Daniel Shalem, Dudu Moshe, Eitan Richardson, Eran Levin, Guy Shiran, Nir Zabari, Ori Gordon, et al. Ltx-video: Realtime video latent diffusion. *arXiv preprint arXiv:2501.00103*, 2024. 1

[12] Dongchen Han, Xuran Pan, Yizeng Han, Shiji Song, and Gao Huang. Flatten transformer: Vision transformer using focused linear attention. In *Proceedings of the IEEE/CVF international conference on computer vision*, pages 5961–5971, 2023. 3

[13] Alex Henry, Prudhvi Raj Dachapally, Shubham Shantaram Pawar, and Yuxuan Chen. Query-key normalization for transformers. In *Findings of the Association for Computational Linguistics: EMNLP 2020*, pages 4246–4253, 2020. 3

[14] Jonathan Ho, William Chan, Chitwan Saharia, Jay Whang, Ruiqi Gao, Alexey Gritsenko, Diederik P Kingma, Ben Poole, Mohammad Norouzi, David J Fleet, et al. Imagen video: High definition video generation with diffusion models. *arXiv preprint arXiv:2210.02303*, 2022. 2

[15] Wenyi Hong, Ming Ding, Wendi Zheng, Xinghan Liu, and Jie Tang. Cogvideo: Large-scale pretraining for text-to-video generation via transformers. *arXiv preprint arXiv:2205.15868*, 2022. 1

[16] Xun Huang, Zhengqi Li, Guande He, Mingyuan Zhou, and Eli Shechtman. Self forcing: Bridging the train-test gap in autoregressive video diffusion. *arXiv preprint arXiv:2506.08009*, 2025. 2, 3, 5

[17] Ziqi Huang, Yinan He, Jiashuo Yu, Fan Zhang, Chenyang Si, Yuming Jiang, Yuanhan Zhang, Tianxing Wu, Qingyang Jin, Nattapol Chanpaisit, Yaohui Wang, Xinyuan Chen, Limin Wang, Dahua Lin, Yu Qiao, and Ziwei Liu. Vbench: Comprehensive benchmark suite for video generative models. In *Proceedings of the IEEE/CVF Conference on Computer Vision and Pattern Recognition*, 2024. 8, 2

[18] Eric Jang, Shixiang Gu, and Ben Poole. Categorical reparameterization with gumbel-softmax. *arXiv preprint arXiv:1611.01144*, 2016. 5

[19] Animesh Karnewar, Denis Korzhenkov, Ioannis Lelekas, Adil Karjauv, Noor Fathima, Hanwen Xiong, Vancheeswaran Vaidyanathan, Will Zeng, Rafael Esteves, Tushar Singhal, et al. Neodragon: Mobile video generation using diffusion transformer. *arXiv preprint arXiv:2511.06055*, 2025. 2

[20] Angelos Katharopoulos, Apoorv Vyas, Nikolaos Pappas, and François Fleuret. Transformers are rnns: Fast autoregressive transformers with linear attention. In *International conference on machine learning*, pages 5156–5165. PMLR, 2020. 3

[21] Bosung Kim, Kyuhwan Lee, Isu Jeong, Jungmin Cheon, Yeojin Lee, and Seulki Lee. On-device sora: Enabling training-free diffusion-based text-to-video generation for mobile devices. 2025. 2

[22] Weijie Kong, Qi Tian, Zijian Zhang, Rox Min, Zuozhuo Dai, Jin Zhou, Jiangfeng Xiong, Xin Li, Bo Wu, Jianwei Zhang, et al. Hunyuanyvideo: A systematic framework for large video generative models. *arXiv preprint arXiv:2412.03603*, 2024. 2, 5

[23] Kuaishou. Kling. <https://kling.kuaishou.com/en>, 2024.

[24] Bin Lin, Yunyang Ge, Xinhua Cheng, Zongjian Li, Bin Zhu, Shaodong Wang, Xianyi He, Yang Ye, Shanghai Yuan, Lihuan Chen, et al. Open-sora plan: Open-source large video

generation model. *arXiv preprint arXiv:2412.00131*, 2024. 2

[25] Shanchuan Lin, Ceyuan Yang, Hao He, Jianwen Jiang, Yuxi Ren, Xin Xia, Yang Zhao, Xuefeng Xiao, and Lu Jiang. Autoregressive adversarial post-training for real-time interactive video generation. 2025. 2, 3, 5

[26] Peter J Liu, Mohammad Saleh, Etienne Pot, Ben Goodrich, Ryan Sepassi, Lukasz Kaiser, and Noam Shazeer. Generating wikipedia by summarizing long sequences. *arXiv preprint arXiv:1801.10198*, 2018. 4

[27] Guoqing Ma, Haoyang Huang, Kun Yan, Liangyu Chen, Nan Duan, Shengming Yin, Changyi Wan, Ranchen Ming, Xiaoniu Song, Xing Chen, et al. Step-video-t2v technical report: The practice, challenges, and future of video foundation model. *arXiv preprint arXiv:2502.10248*, 2025. 2

[28] Willi Menapace, Aliaksandr Siarohin, Ivan Skorokhodov, Ekaterina Deyneka, Tsai-Shien Chen, Anil Kag, Yuwei Fang, Aleksei Stoliar, Elisa Ricci, Jian Ren, et al. Snap video: Scaled spatiotemporal transformers for text-to-video synthesis. *arXiv preprint arXiv:2402.14797*, 2024. 2

[29] Kepan Nan, Rui Xie, Penghao Zhou, Tiehan Fan, Zhenheng Yang, Zhijie Chen, Xiang Li, Jian Yang, and Ying Tai. Openvid-1m: A large-scale high-quality dataset for text-to-video generation. *ArXiv preprint*, abs/2407.02371, 2024. 6

[30] OpenAI. Video generation models as world simulators. <https://openai.com/index/video-generation-models-as-world-simulators/>, 2023. 2

[31] Adam Polyak, Amit Zohar, Andrew Brown, Andros Tjandra, Animesh Sinha, Ann Lee, Apoorv Vyas, Bowen Shi, Chih-Yao Ma, Ching-Yao Chuang, et al. Movie gen: A cast of media foundation models. *arXiv preprint arXiv:2410.13720*, 2024. 2

[32] Adam Polyak, Amit Zohar, Andrew Brown, Andros Tjandra, Animesh Sinha, Ann Lee, Apoorv Vyas, Bowen Shi, Chih-Yao Ma, Ching-Yao Chuang, et al. Movie gen: A cast of media foundation models. *ArXiv preprint*, abs/2410.13720, 2024. 3

[33] Zhen Qin, Weixuan Sun, Hui Deng, Dongxu Li, Yunshen Wei, Baohong Lv, Junjie Yan, Lingpeng Kong, and Yiran Zhong. cosformer: Rethinking softmax in attention. *arXiv preprint arXiv:2202.08791*, 2022. 3

[34] Alec Radford, Jong Wook Kim, Chris Hallacy, Aditya Ramesh, Gabriel Goh, Sandhini Agarwal, Girish Sastry, Amanda Askell, Pamela Mishkin, Jack Clark, et al. Learning transferable visual models from natural language supervision. In *International conference on machine learning*, pages 8748–8763. PMLR, 2021. 6

[35] Jianlin Su, Murtadha Ahmed, Yu Lu, Shengfeng Pan, Wen Bo, and Yunfeng Liu. Roformer: Enhanced transformer with rotary position embedding. *Neurocomputing*, 568:127063, 2024. 3, 1

[36] Xingwu Sun, Yanfeng Chen, Yiqing Huang, Ruobing Xie, Jiaqi Zhu, Kai Zhang, Shuaipeng Li, Zhen Yang, Jonny Han, Xiaoobo Shu, et al. Hunyuan-large: An open-source moe model with 52 billion activated parameters by tencent. *arXiv preprint arXiv:2411.02265*, 2024. 1

[37] Genmo Team. Mochi, 2024. 2

[38] Gemma Team, Aishwarya Kamath, Johan Ferret, Shreya Pathak, Nino Vieillard, Ramona Merhej, Sarah Perrin, Tatiana Matejovicova, Alexandre Ramé, Morgane Rivière, et al. Gemma 3 technical report. *arXiv preprint arXiv:2503.19786*, 2025. 6

[39] Team Wan, Ang Wang, Baole Ai, Bin Wen, Chaojie Mao, Chen-Wei Xie, Di Chen, Feiwu Yu, Haiming Zhao, Jianxiao Yang, Jianyuan Zeng, Jiayu Wang, Jingfeng Zhang, Jingen Zhou, Jinkai Wang, Jixuan Chen, Kai Zhu, Kang Zhao, Keyu Yan, Lianghua Huang, Mengyang Feng, Ningyi Zhang, Pandeng Li, Pingyu Wu, Ruihang Chu, Ruili Feng, Shiwei Zhang, Siyang Sun, Tao Fang, Tianxing Wang, Tianyi Gui, Tingyu Weng, Tong Shen, Wei Lin, Wei Wang, Wei Wang, Wenmeng Zhou, Wente Wang, Wenting Shen, Wenyan Yu, Xianzhong Shi, Xiaoming Huang, Xin Xu, Yan Kou, Yangyu Lv, Yifei Li, Yijing Liu, Yiming Wang, Yingya Zhang, Yitong Huang, Yong Li, You Wu, Yu Liu, Yulin Pan, Yun Zheng, Yuntao Hong, Yupeng Shi, Yutong Feng, Zeyinzi Jiang, Zhen Han, Zhi-Fan Wu, and Ziyu Liu. Wan: Open and advanced large-scale video generative models. 2025. 2

[40] Team Wan, Ang Wang, Baole Ai, Bin Wen, Chaojie Mao, Chen-Wei Xie, Di Chen, Feiwu Yu, Haiming Zhao, Jianxiao Yang, et al. Wan: Open and advanced large-scale video generative models. *arXiv preprint arXiv:2503.20314*, 2025. 1, 2, 5, 6, 7, 3

[41] Fu-Yun Wang, Zhaoyang Huang, Xiaoyu Shi, Weikang Bian, Guanglu Song, Yu Liu, and Hongsheng Li. Animatelcm: Accelerating the animation of personalized diffusion models and adapters with decoupled consistency learning. *ArXiv preprint*, abs/2402.00769, 2024. 1

[42] Fu-Yun Wang, Ling Yang, Zhaoyang Huang, Mengdi Wang, and Hongsheng Li. Rectified diffusion: Straightness is not your need in rectified flow. *arXiv preprint arXiv:2410.07303*, 2024. 5

[43] Wenhui Wang, Enze Xie, Xiang Li, Deng-Ping Fan, Kaitao Song, Ding Liang, Tong Lu, Ping Luo, and Ling Shao. Pyramid vision transformer: A versatile backbone for dense prediction without convolutions. In *Proceedings of the IEEE/CVF international conference on computer vision*, pages 568–578, 2021. 4

[44] Jay Zhangjie Wu, Yixiao Ge, Xintao Wang, Stan Weixian Lei, Yuchao Gu, Yufei Shi, Wynne Hsu, Ying Shan, Xiaohu Qie, and Mike Zheng Shou. Tune-a-video: One-shot tuning of image diffusion models for text-to-video generation. In *Proceedings of the IEEE/CVF international conference on computer vision*, pages 7623–7633, 2023. 1

[45] Yushu Wu, Yanyu Li, Anil Kag, Ivan Skorokhodov, Willi Menapace, Ke Ma, Arpit Sahni, Ju Hu, Aliaksandr Siarohin, Dhritiman Sagar, Yanzhi Wang, and Sergey Tulyakov. Taming diffusion transformer for efficient mobile video generation in seconds. 2025. 1, 2, 4, 5

[46] Yushu Wu, Zhixing Zhang, Yanyu Li, Yanwu Xu, Anil Kag, Yang Sui, Huseyin Coskun, Ke Ma, Aleksei Lebedev, Ju Hu, et al. Snapgen-v: Generating a five-second video within five seconds on a mobile device. In *Proceedings of the Computer Vision and Pattern Recognition Conference*, pages 2479–2490, 2025. 1, 2

[47] Haocheng Xi, Shuo Yang, Yilong Zhao, Chenfeng Xu, Muyang Li, Xiuyu Li, Yujun Lin, Han Cai, Jintao Zhang, Dacheng Li, et al. Sparse videogen: Accelerating video diffusion transformers with spatial-temporal sparsity. *arXiv preprint arXiv:2502.01776*, 2025. 3

[48] Enze Xie, Junsong Chen, Junyu Chen, Han Cai, Haotian Tang, Yujun Lin, Zhekai Zhang, Muyang Li, Ligeng Zhu, Yao Lu, et al. Sana: Efficient high-resolution image synthesis with linear diffusion transformers. *arXiv preprint arXiv:2410.10629*, 2024. 3, 6

[49] Enze Xie, Junsong Chen, Junyu Chen, Han Cai, Haotian Tang, Yujun Lin, Zhekai Zhang, Muyang Li, Ligeng Zhu, Yao Lu, et al. Sana: Efficient high-resolution image synthesis with linear diffusion transformers. *arXiv preprint arXiv:2410.10629*, 2024. 3

[50] Haitam Ben Yahia, Denis Korzhenkov, Ioannis Lelekas, Amir Ghodrati, and Amirhossein Habibian. Mobile video diffusion. 2024. 2

[51] Zhuoyi Yang, Jiayan Teng, Wendi Zheng, Ming Ding, Shiyu Huang, Jiazheng Xu, Yuanming Yang, Wenyi Hong, Xiaohan Zhang, Guanyu Feng, et al. Cogvideox: Text-to-video diffusion models with an expert transformer. *arXiv preprint arXiv:2408.06072*, 2024. 2

[52] Tianwei Yin, Michaël Gharbi, Taesung Park, Richard Zhang, Eli Shechtman, Fredo Durand, and William T Freeman. Improved distribution matching distillation for fast image synthesis. *ArXiv preprint, abs/2405.14867*, 2024. 2

[53] Tianwei Yin, Qiang Zhang, Richard Zhang, William T Freeman, Fredo Durand, Eli Shechtman, and Xun Huang. From slow bidirectional to fast autoregressive video diffusion models. In *CVPR*, 2025. 2, 3

[54] Zhixing Zhang, Yanyu Li, Yushu Wu, yanwu xu, Anil Kag, Ivan Skorokhodov, Willi Menapace, Aliaksandr Siarohin, Junli Cao, Dimitris N. Metaxas, Sergey Tulyakov, and Jian Ren. SF-v: Single forward video generation model. In *The Thirty-eighth Annual Conference on Neural Information Processing Systems*, 2024. 2

[55] Wenliang Zhao, Lujia Bai, Yongming Rao, Jie Zhou, and Jiwen Lu. Unipc: A unified predictor-corrector framework for fast sampling of diffusion models. *Advances in Neural Information Processing Systems*, 36:49842–49869, 2023. 6

[56] Zangwei Zheng, Xiangyu Peng, Tianji Yang, Chenhui Shen, Shenggui Li, Hongxin Liu, Yukun Zhou, Tianyi Li, and Yang You. Open-sora: Democratizing efficient video production for all, 2024. 1, 2

[57] Shangchen Zhou, Peiqing Yang, Jianyi Wang, Yihang Luo, and Chen Change Loy. Upscale-a-video: Temporal-consistent diffusion model for real-world video super-resolution. In *Proceedings of the IEEE/CVF Conference on Computer Vision and Pattern Recognition*, pages 2535–2545, 2024. 1

[58] Yuan Zhou, Qiuyue Wang, Yuxuan Cai, and Huan Yang. Allegro: Open the black box of commercial-level video generation model. *arXiv preprint arXiv:2410.15458*, 2024. 6

S²DiT: Sandwich Diffusion Transformer for Mobile Streaming Video Generation

Supplementary Material

A. Search algorithm

We provide the detailed search algorithm as follows Algorithm 1. Moreover, we adopt design improvements that dramatically reduce computation and yield higher training efficiency.

Efficient Search Space Formulation. We reduce the search space in three ways: (i) We use group-wise rather than block-wise masking, yielding an exponential reduction in the search space. With two blocks per group, the space reduces from $2^{(2n)}$ to 2^n . (ii) We set $m_1 = m_M = 1$ to make the spatial scale matches the VAE compression ratio, further reducing the space to $2^{(n-2)}$. (iii) Base on the dynamic programming, we fix the counts of groups assigned to LCHA (k) and SSA ($n-k-2$) in the search space, reducing the space from $2^{(n-2)}$ to C_{n-2}^k . Overall, these choices reduce the space from $2^{(2n)}$ to C_{n-2}^k , yielding a substantially more efficient and well-structured search algorithm.

Algorithm 1 Sandwich Architecture Search Algorithm

```

1: Input: Input feature  $y$ , groups  $M$ , group modules
    $\{f_L^n, f_S^n\}_{n=1}^M$ , upsampler  $up_n(\cdot)$ , downampler  $down_n(\cdot)$ 

2: Learnable: Binary routers  $\{m_n\}_{n=1}^M$  (trained via Gumbel-Softmax + STE)
3: Output: Output feature  $\hat{y}$ 
4: Initialize  $y_L^0 \leftarrow y$ ,  $y_S^0 \leftarrow down_1(y)$ 
5: Initialize  $S^0 \leftarrow 0$ 
6: Initialize  $m_0 \leftarrow 1$ 
7: for  $n = 1$  to  $M$  do
   // Branch-Switch Triggers
8:    $u_n \leftarrow \max\{m_n - m_{n-1}, 0\}$ 
9:    $d_n \leftarrow \max\{m_{n-1} - m_n, 0\}$ 
   // Prepare Inputs for Group  $n$ 
10:   $x_L^n \leftarrow (1 - u_n) y_L^{n-1} + u_n \cdot (up_n(y_S^{n-1}) + S^{n-1})$ 
11:   $x_S^n \leftarrow (1 - d_n) y_S^{n-1} + d_n \cdot down_n(y_L^{n-1})$ 
   // Per-Group Forward
12:   $\tilde{y}_L^n \leftarrow f_L^n(x_L^n)$ 
13:   $\tilde{y}_S^n \leftarrow f_S^n(x_S^n)$ 
   // Update Long-Skip Buffer
14:   $S^n \leftarrow d_n \cdot y_L^{n-1} + (1 - d_n) \cdot S^{n-1}$ 
   // Differentiable Routing via
   // Gumbel-Softmax + STE
15:   $y_L^n \leftarrow m_n \cdot \tilde{y}_L^n + (1 - m_n) \cdot y_L^{n-1}$ 
16:   $y_S^n \leftarrow (1 - m_n) \cdot \tilde{y}_S^n + m_n \cdot y_S^{n-1}$ 
17: end for
   // Final Merge
18:  $\hat{y} \leftarrow m_M \cdot y_L^{(M)} + (1 - m_M) \cdot up_M(y_S^{(M)})$ 
19: return  $\hat{y}$ 

```

Efficient training design. We replace costly pre-training

with self-distillation to achieve efficient training, as expressed as:

$$\mathcal{L}_{sd} = \mathbb{E} \left[\|\hat{y} - T_\theta(y_L^1)\|_2^2 \right], \quad (10)$$

where \mathcal{L}_{sd} is the self-distillation loss, $T_\theta(\cdot)$ denotes the pre-trained teacher model with all self-attention blocks. For the student model, we initialize the LCHA and SSA by inheriting parameters from $T_\theta(\cdot)$ wherever compatible. Since both LCHA and SSA are variants of self-attention, most parameters are transferable, yielding a more efficient training setup.

B. Model Design

RoPE-3D. We follow RoPE [35] to incorporate rotary position embeddings into the linear attention formulation, as shown in Eq. (11). As discussed in [35], RoPE injects position while keep norm unchanged. Therefore, the RoPE transformation is applied only to the outputs of non-linear functions. Meanwhile, the denominator remains unchanged to avoid potential division-by-zero issues.

$$\text{Attn}(\mathbf{Q}, \mathbf{K}, \mathbf{V})_m = \frac{\sum_{n=1}^N (\mathbf{R}_{\Theta, m}^d \phi(\mathbf{q}_m))^\top (\mathbf{R}_{\Theta, n}^d \varphi(\mathbf{k}_n)) \mathbf{v}_n}{\sum_{n=1}^N \phi(\mathbf{q}_m)^\top \varphi(\mathbf{k}_n)}. \quad (11)$$

Normalization. We employ Layer Normalization in transformer blocks and also as QK norm. In mobile deployment we identify that RMS norm yields higher numeric error, as a result, we use LayerNorm with affine transformation instead. We use AdaLN as timestep encoding which follows common practices [10, 40].

C. More details for 2-in-1 Distillation

C.1. Details of Offline Cached Knowledge Distillation.

After evaluating visual fidelity across several candidates, we adopt Wan2.2-14B [40] as the teacher. A key challenge is Wan2.2's Mixture-of-Experts design, with separate high-noise and low-noise experts, which makes on-the-fly distillation computationally prohibitive. We provide the details of our distillation procedure here.

We propose *Offline Cached Knowledge Distillation*, an offline two-stage protocol: (i) *Cache stage*: for the teacher model, we precompute and cache text embedding e_t , the diffusion tuple of timestep, noise, and velocity of high noise expert (t_h, n_h, v_h) and low noise expert (t_l, n_l, v_l) . (ii) *Distillation stage*: during distillation, the training only uses

# Steps	DD	OC	AQ	Quality	Semantic	Total
1	55.09	85.42	52.85	82.80	70.65	80.37
2	57.50	91.25	64.04	85.08	73.15	82.69
4	59.17	89.49	65.64	85.26	73.79	83.26

Table A1. Analysis of the number of inference steps. We measure VBFN [17] score with different numbers of inference steps. In the results, “DD”, “OC”, and “AQ” denote the dynamic degree, object class, and aesthetic quality scores, respectively.

cached tuples and skips teacher forward passes, which substantially reduces both FLOPs and peak memory. The process can be formally defined by:

$$\mathcal{L}_{\text{KD}} = \mathbb{E} \left[w_l \|v_l - V_\theta(t_l, n_l, e_l)\|_2^2 + w_h \|v_h - V_\theta(t_h, n_h, e_h)\|_2^2 \right], \quad (12)$$

where $V_\theta(\cdot)$ indicates the predicted velocity of our model, w_l and w_h are the hyper-parameter to adjust the weight between the two experts.

We set $w_l = w_h = 0.5$ in our experiments.

C.2. Details of Self-Forcing Distillation.

Self-Forcing [16] fine-tuning pipeline has shown promising results for 4-step auto-regressive generation. However, its performance tends to degrade significantly when applied to fewer steps (e.g., 1-step or 2-step generation). A common approach to address this issue is adversarial fine-tuning, which aims to enhance quality in low-step generation. Nonetheless, adversarial fine-tuning often suffers from training instability due to the substantial gap between “real” and “fake” samples, since previous works [46, 52, 54] typically use real-world data as the “real” samples. To mitigate the misalignment, a more intuitive strategy is to adopt progressive adversarial fine-tuning, where samples generated with more sampling steps are treated as the “real” samples instead of real-world data. Following backward simulation [52], we denote $x_{0:T}$ and $x_{0:T'}$ as the x_0 predictions obtained with T and T' sampling steps, respectively, where $T < T'$. In this setting, $x_{0:T}$ serves as the “fake” sample and $x_{0:T'}$ as the “real” sample. Inspired by R3GAN, we employ the RpGAN+ $R_1 + R_2$ formulation as the adversarial fine-tuning objective:

$$R_1(\psi) = \frac{\gamma}{2\epsilon} \mathbb{E} [\mathcal{D}(x_{t;T'} + \epsilon) - \mathcal{D}(x_{t;T'})], \quad (13)$$

$$R_2(\psi) = \frac{\gamma}{2\epsilon} \mathbb{E} [\mathcal{D}(x_{t;T} + \epsilon) - \mathcal{D}(x_{t;T})], \quad (14)$$

$$\mathcal{L}_{\text{adv}}^{\mathcal{D}} = \mathbb{E} [\text{softplus}(-(\mathcal{D}(x_{t;T'}) - \mathcal{D}(x_{t;T})))],$$

$$\mathcal{L}_{\text{adv}}^{\mathcal{G}} = \mathbb{E} [\text{softplus}(\mathcal{D}(x_{t;T'}) - \mathcal{D}(x_{t;T}))],$$

where the $x_{t;T'}$ and $x_{t;T}$ are noisy latent that backward simulated with T and T' sampling step added by t noise-level.

Training details. We adopt the AdamW optimizer for the generator and discriminator, using a learning rate of $1.0e-5$ for the generator and $2.0e-6$ for the discriminator with betas set to $[0, 0.999]$. An exponential moving average (EMA) with a decay rate of 0.99 is also applied to the generator for improved training stability.

Evaluation on inference-step. We provide the performance of different inference step in Tab. A1. A single step already delivers surprisingly strong results with 80.37 total score, indicating that most of the global structure and appearance can be formed in one-step. Besides, the two-step setting provides the best speed-quality trade-off and the most stable behavior across metrics. Finally, increasing to four steps further improves accuracy, reaching the highest score (83.26) with acceptable latency.

D. Details of Mobile Deployment

D.1. Efficient Decoder

We freeze the VAE encoder of Wan2.1 and train an efficient decoder that decodes in real-time on mobile, as shown in (Tab. A2). We build the efficient decoder with narrow 3D convolutions, group normalizations, and use Hardswish as the activation function. We encode video data with Wan2.1 encoder and obtain the latents, and the efficient decoder is trained to reconstruct the video with L1 loss, Perceptual loss and GAN loss. Our efficient decoder is $4\times$ smaller in size and can decode beyond real time on mobile, while still deliver on-par reconstruction quality.

Decoder	Params.	Latency	PSNR	SSIM	FVD
Wan 2.1	60M	oom	32.16	0.8856	23.9
Ours	14M	80ms	31.71	0.8788	27.1

Table A2. Mobile efficient decoder for real-time decoding.

D.2. Deployment Details and Speed Benchmark

We provide a latency breakdown in Tab. A3. In the case of mobile deployment, we solely use CLIP-ViT-L as the text encoder. We generate 3 latent frames for each chunk, and use a window size of 2 for KV cache. We deploy the model with Apple CoreMLtools [1], with the VAE decoder running on GPU and S²DiT running on neural engine to maximize resource utilization. We follow official practice [1] to deploy S²DiT with 8-bit activation quantization and mixed-precision quantization for weights. Specifically, we keep sensitive layers (e.g., project in and out layers, text embedding layers) in 8-bit, but put most other layers in 4-bit. With deploy-time calibration, we observe minimal quality drop compared to the server BF16 model.

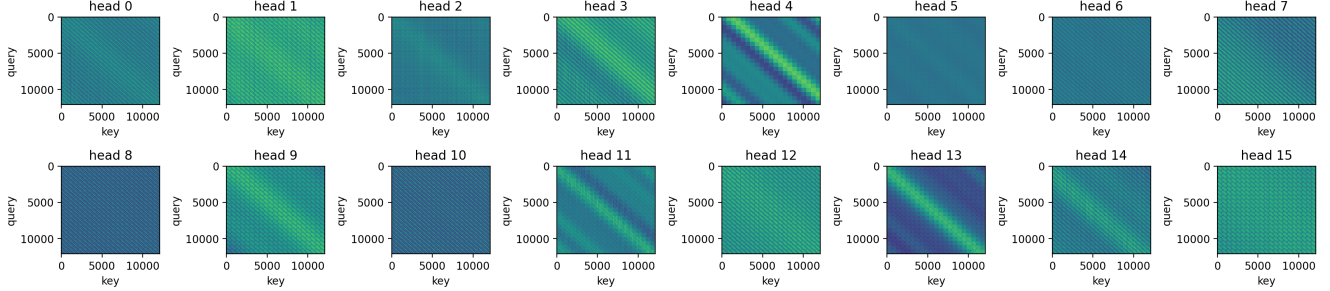


Figure A1. Visualization of attention maps from our proposed linear attention.

Model:	S ² DiT-Pre.	Wan2.1-1.3B	LTX-0.9.5
Text Alignment	49.80%	47.39%	2.81%
Overall Quality	46.99%	43.37%	9.64%
Model:	S ² DiT-KD	Wan2.1-1.3B	LTX-0.9.5
Text Alignment	61.45%	36.66%	1.89%
Overall Quality	54.30%	36.29%	9.41%
Model:	S ² DiT-AR	Wan2.1-1.3B	LTX-0.9.5
Text Alignment	60.08%	37.48%	2.44%
Overall Quality	57.39%	35.62%	6.99%

Table A4. User study on 250 Randomly Selected Prompts from MovieGen VideoBench [32]. We show the win rate of each model.

Model	Latency (ms)	Steps
Text Encoder	4	1
S ² DiT	260	4
Decoder	80	1
Total	1124	FPS:10.7

Table A3. Latency breakdown for generating a single chunk with 3 latent frames, which will be decoded to 12 pixel frames.

E. User Study

We perform a user study of text-to-video generation on 250 randomly sampled MovieGen VideoBench [32] prompts. We compare the S²DiT-pretrained model, knowledge distilled model (KD), and autoregressive model (AR) with two baseline models, i.e., Wan2.1 1.3B [40] and LTX-0.9.5 [10]. Human labelers are asked to pick the best from three anonymous and randomly shuffled videos. We instruct human labelers to focus on two metrics, (i) Text alignment, which evaluates whether the generated video follows the provided input prompt. (ii) Overall Quality, whether the generated video is visually pleasing, i.e., has complete generated object, meaningful and smooth motion, less flickering and artifacts, etc. Each metric is evaluated by at least 5 labelers

and we take the average win rate. We find that with the detailed instruction, the variance of the picked results from different human labelers is generally low (< 3% difference in win rate).

As in Tab. A4, we show that our base model achieves on-par performance with the server-SOTA Wan2.1 1.3B model [40], and outperforms server-efficient LTX [10] by a large margin, demonstrating the superior performance of the proposed Sandwich Diffusion Transformer. With the subsequent 2-in-1 distillation, our KD full step model and streaming generation model achieves even higher win rate. We are the first to demonstrate high-quality streaming video generation but with mobile budget.

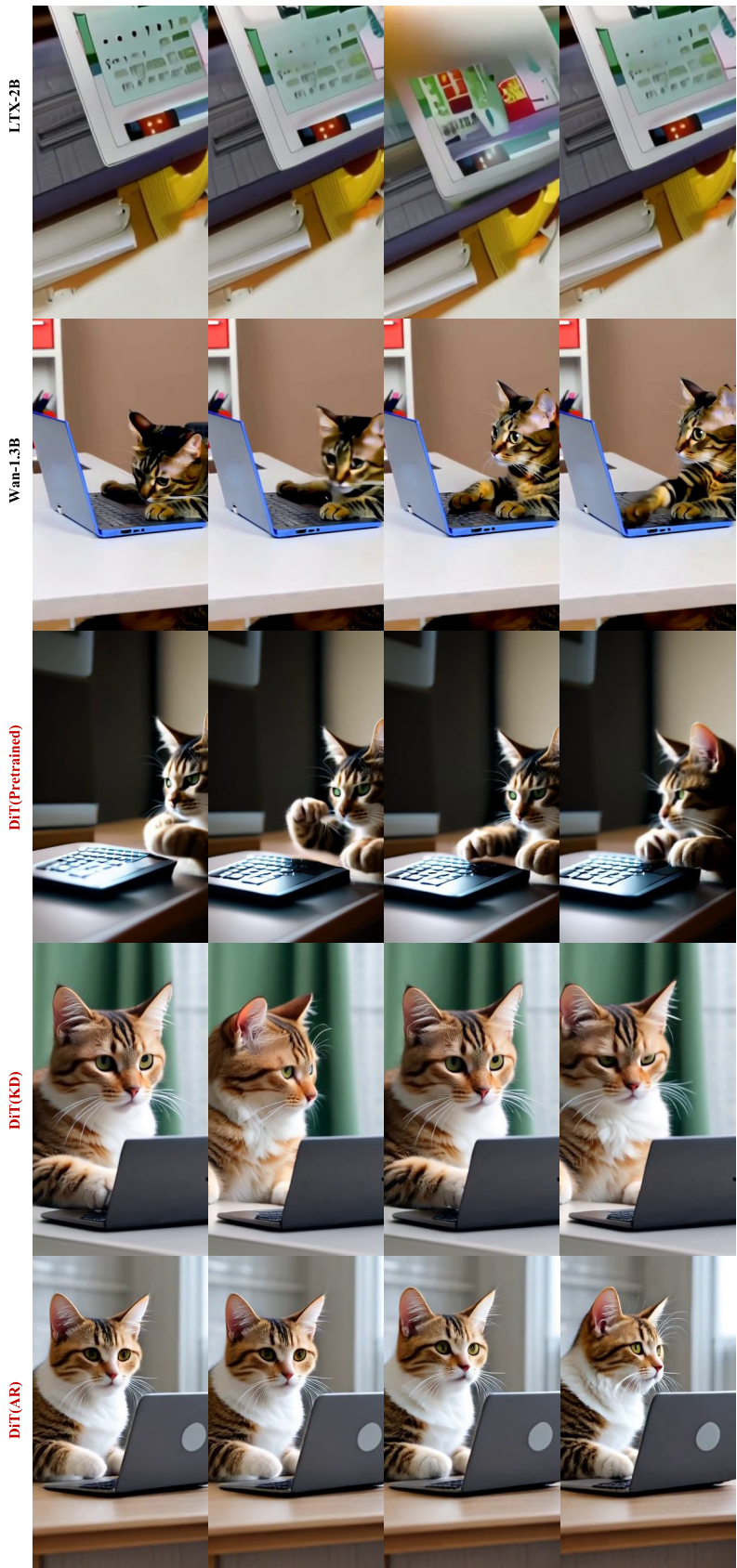
F. Analysis of Linear Attention

We visualize the attention maps produced by our linear-attention module. As shown in Fig. A1, the heads exhibit clear specialization: some emphasize temporal dynamics (e.g., heads 12 and 15), while others focus on spatial structure (e.g., heads 4 and 13), consistent with prior observations for self-attention [47].

Besides, several heads capture global context (e.g., heads 2 and 5). In conjunction with the local path, this combination enables our model to learn global context and local detail simultaneously. Consistent with this, our full model consistently outperforms the Local path-only variant across all evaluation metrics as illustrated in Tab. 3, confirming the importance of combining global and local.

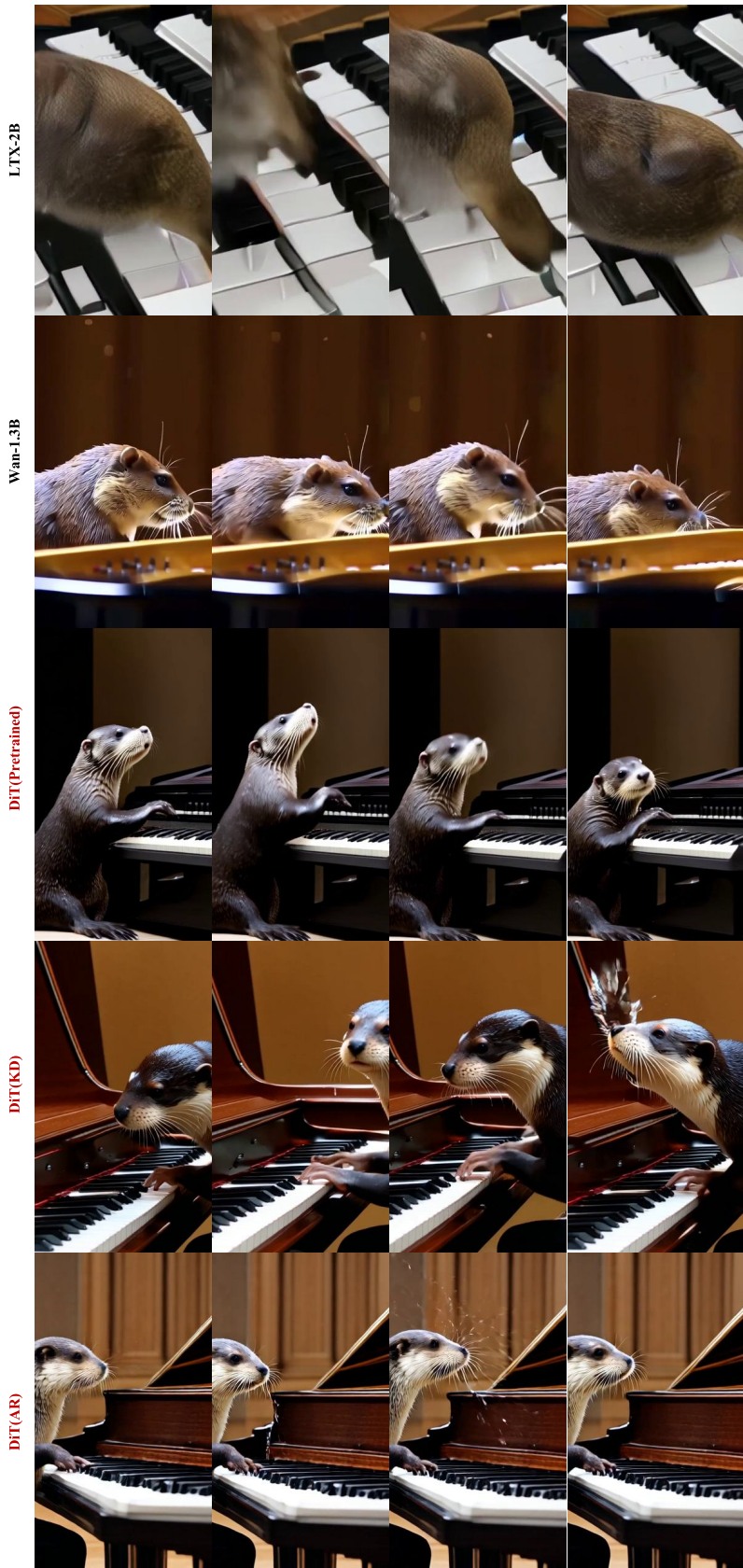
G. More Visualizations

Beyond the horizontal results reported in the main paper, we include the comparisons of vertical videos that demonstrate the effectiveness of S²DiT. As shown in Figs. A2 to A4, S²DiT variants achieves stronger text-video alignment and richer visual details. We include more videos and comparisons in the media file.



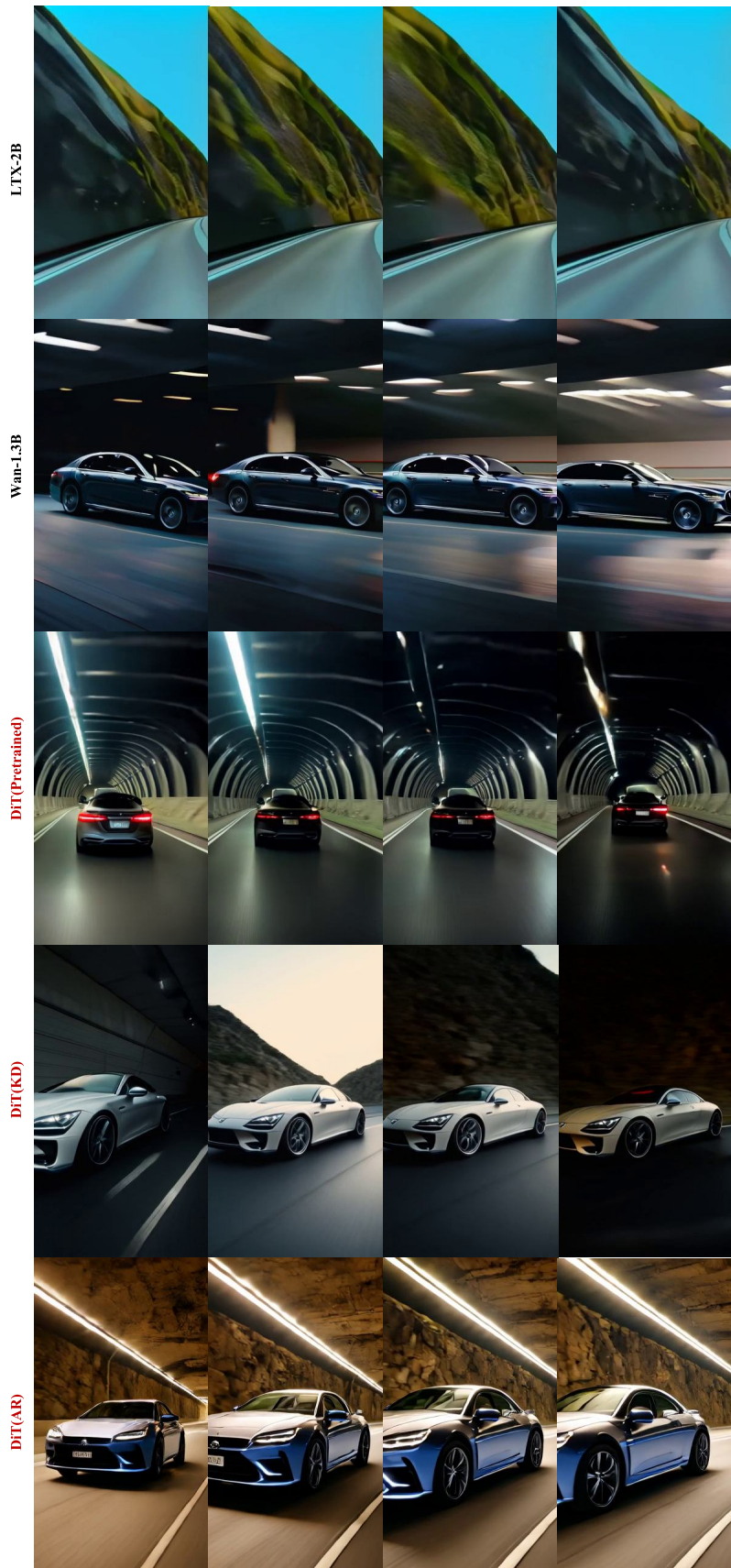
Prompt: In a well-appointed study, a cat sits behind a desk, 'typing' on a miniature laptop. ... the keyboard....

Figure A2. Qualitative comparison on vertical videos.



Prompt: In a grand concert hall, focus on an otter gracefully playing a piano with remarkable skill...

Figure A3. Qualitative comparison on vertical videos.



Prompt: A luxury car elegantly cruises through a well-lit mountain tunnel. Cinematic tracking shot...

Figure A4. Qualitative comparison on vertical videos.